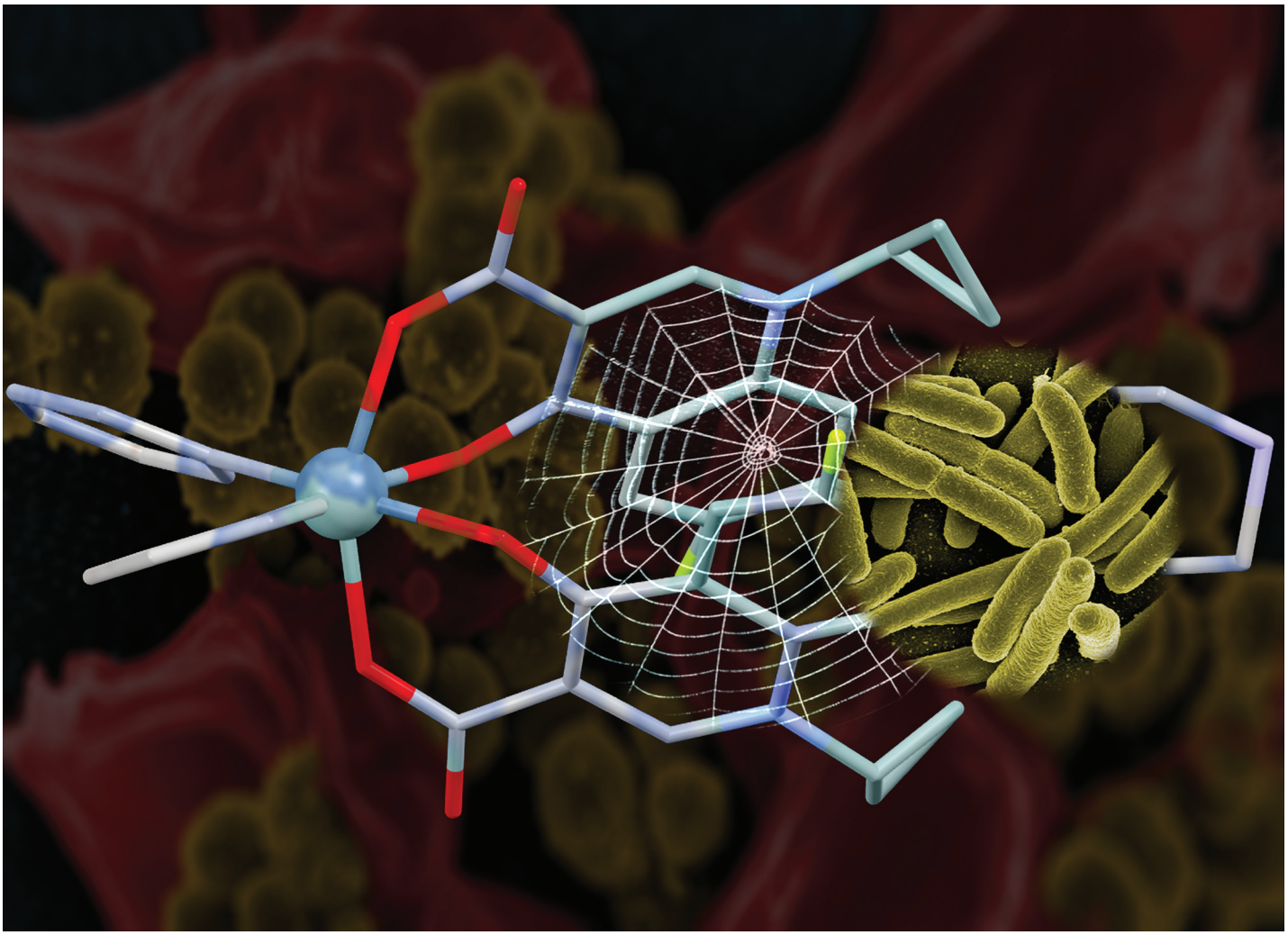

Showcasing research from the Biological Inorganic Chemistry Laboratory (Prof. Sotiris K. Hadjikakou) of the Department of Chemistry in the University of Ioannina, Greece.

Ciprofloxacin conjugated to diphenyltin(IV): a novel formulation with enhanced antimicrobial activity

The stereoisomer Δ-*cis*-[$Ph_2Sn(CIP)_2$] (**CIPTIN**) was obtained from ciprofloxacin and diphenyltin dichloride. 2D layer supramolecular assembly is established based on strong hydrogen bonding interactions. **CIPTIN** eliminates both Gram-positive and Gram-negative bacteria tested, and is stronger than the ciprofloxacin itself.

As featured in:

See C. N. Banti, S. K. Hadjikakou *et al.*, *Dalton Trans.*, 2020, **49**, 11522.

ROYAL SOCIETY OF CHEMISTRY

rsc.li/dalton

Registered charity number: 207890

Dalton Transactions

ROYAL SOCIETY OF CHEMISTRY

PAPER

View Article Online
View Journal | View Issue

Cite this: *Dalton Trans.*, 2020, **49**, 11522

Ciprofloxacin conjugated to diphenyltin(IV): a novel formulation with enhanced antimicrobial activity†

M. P. Chrysouli,[a] C. N. Banti, *[a] N. Kourkoumelis,[b] E. E. Moushi,[c] A. J. Tasiopoulos, [d] A. Douvalis,[e] C. Papachristodoulou,[f] A. G. Hatzidimitriou,[g] T. Bakas[e] and S. K. Hadjikakou *[a,h]

The metalloantibiotic of formula $Ph_2Sn(CIP)_2$ (**CIPTIN**) (**HCIP** = ciprofloxacin) was synthesized by reacting ciprofloxacin hydrochloride (**HCIP·HCl**) (an antibiotic in clinical use) with diphenyltin dichloride (Ph_2SnCl_2 **DPTD**). The complex was characterized in the solid state by melting point, FT-IR, X-ray Powder Diffraction (XRPD) analysis, ^{119}Sn Mössbauer spectroscopy, X-ray Fluorescence (XRF) spectroscopy, and Thermogravimetry/Differential Thermal Analysis (TG-DTA) and in solution by UV-Vis, ^{1}H NMR spectroscopic techniques and Electrospray Ionisation Mass Spectrometry (ESI-MS). The crystal structure of **CIPTIN** and its processor **HCIP** was also determined by X-ray crystallography.

The antibacterial activity of **CIPTIN**, **HCIP·HCl**, **HCIP** and **DPTD** was evaluated against the bacterial species *Pseudomonas aeruginosa* (*P. aeruginosa*), *Escherichia coli* (*E. coli*), *Staphylococcus aureus* (*S. aureus*) and *Staphylococcus epidermidis* (*S. epidermidis*), by the means of Minimum Inhibitory Concentration (MIC), Minimum Bactericidal Concentration (MBC) and Inhibition Zones (IZs). **CIPTIN** shows lower MIC values than those of **HCIP·HCl** (up to 4.2-fold), **HCIP** (up to 2.7-fold) or **DPTD** (>135-fold), towards the tested microbes. **CIPTIN** is classified into bactericidal agents according to MBC/MIC values. The developing IZs are 40.8 ± 1.5, 34.0 ± 0.8, 36.0 ± 1.1 and 42.7 ± 0.8 mm, respectively which classify the microbes *P. aeruginosa*, *E. coli*, *S. aureus* and *S. epidermidis* to susceptible ones to **CIPTIN**. These IZs are greater than the corresponding ones of **HCIP·HCl** by 1.1 to 1.5-fold against both the tested Gram negative and Gram positive bacteria. **CIPTIN** eradicates the biofilm of *P. aeruginosa* and *S. aureus* more efficiently than **HCIP·HCl** and **HCIP**. The *in vitro* toxicity and genotoxicity of **CIPTIN** were tested against human skin keratinocyte cells (HaCaT) (IC_{50} = 2.33 μM). **CIPTIN** exhibits 2 to 9-fold lower MIC values than its IC_{50} against HaCaT, while its genotoxic effect determined by micronucleus assay is equivalent to the corresponding ones of **HCIP·HCl** or **HCIP**.

Received 7th May 2020,
Accepted 26th June 2020

DOI: 10.1039/d0dt01665a

rsc.li/dalton

Introduction

Ciprofloxacin, a second-generation fluoroquinolone, is effective against both Gram-positive and Gram-negative pathogenic bacteria.[1] It exhibits good bioavailability or tissue permeability, low incidence of toxic effects and bacteriostatic activity.[2] Generally, bacteriocidal agents are preferred than bacteriostatic ones, against infections, since they limit the development of resistance towards bacteria.[3] However, microbes such as *P. aeruginosa*, *E. coli*, *S. aureus* and *S. epidermidis* are reported to have developed resistance towards ciprofloxacin.[4] Hence, efforts were made in recent years to modify ciprofloxacin with metal ions, in order to increase its antibacterial activity against resistant strains.[5–8]

The conjugation of metals with drugs (CoMeDs) is a new research area being investigated for discovery of new synergistic therapeutic modalities. The term "conjugation" is used for polymeric drug formulations, to emphasize the synergistic

[a]*Inorganic and Analytical Chemistry, Department of Chemistry, University of Ioannina, 45110 Ioannina, Greece. E-mail: cbanti@uoi.gr, shadjika@uoi.gr; Tel: x30-26510-08374, x30-26510-08362*
[b]*Medical Physics Laboratory, Medical School, University of Ioannina, Ioannina, Greece*
[c]*Department of Life Sciences, The School of Sciences, European University Cyprus, Nicosia, Cyprus*
[d]*Department of Chemistry, University of Cyprus, 1678 Nicosia, Cyprus*
[e]*Mössbauer Spectroscopy and Physics of Material Laboratory, Department of Physics, University of Ioannina, Ioannina, Greece*
[f]*Department of Physics, University of Ioannina, Ioannina, Greece*
[g]*Department of Chemistry, Aristotle University of Thessaloniki, Thessaloniki, Greece*
[h]*University Research Center of Ioannina (URCI), Institute of Materials Science and Computing, Ioannina, Greece*

†Electronic supplementary information (ESI) available. CCDC 1993746 and 2002394. For ESI and crystallographic data in CIF or other electronic format see DOI: 10.1039/D0DT01665A

effect of a metal with a drug.[9,10] CoMeDs combines metals with specific classes of drugs aiming to create new agents possessing altogether new properties than with the drugs from which they were prepared.[9,10] From this point of view, organotin(IV) compounds which contain active drugs as ligands are expected to exhibit enhanced effectiveness due to the synergy which is developing between the R_nSn(IV) (R = alkyl or aryl group; n = 1 to 3) moiety and the drug. Besides, organotin compounds are commercially used as agricultural biocides.[11,12] Recently, Pokharia *et al.* have shown that triorganotin(IV) complexes of ciprofloxacin (R_3Sn(CIP) (R = Me-, Cy-)) exhibit better antibacterial effect than free ciprofloxacin against *E. faecalis*, *S. aureus*, *K. pneumoniae*, *E. coli*, *P. aeruginosa*, and *P. mirabilis*.[13]

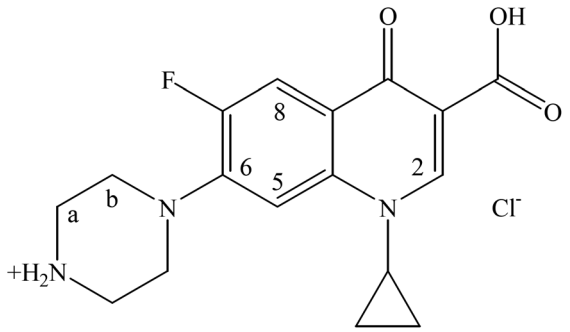

Scheme 1 Schematic illustration of the used ligand hydrochloride ciprofloxacin.

With the aim to develop new antimicrobial agents with enhanced activity capable of overcoming bacterial resistance,[9,10,14–17] the metalloantibiotic of ciprofloxacin (**HCIP**, Scheme 1) having the formula $Ph_2Sn(CIP)_2$ (**CIPTIN**) was synthesized, characterized and evaluated against bacterial strains *P. aeruginosa*, *E. coli*, *S. aureus* and *S. epidermidis*. Moreover, the combination of an antibiotic, ciprofloxacin, which possesses pharmacological significance, and a metal with known biological activity, tin(IV), is expected to throw light on principles that govern the synergy between metals and drugs in these metallodrugs.

Results and discussion

General aspects

A solution of **HCIP·HCl** in water was initially treated with an excess amount of KOH in a 1 : 1.5 molar ratio to form **KCIP**. A solution of **DPTD** (Ph_2SnCl_2, diphenyltin dichloride) in MeOH (1 : 2 metal to **KCIP**) was added to the previous one under continuous stirring for 30 min, (Scheme 2) and the suspension was filtered off.

Crystals of **CIPTIN** were grown by slow evaporation of ddH_2O/MeOH solution. Besides, crystals of **HCIP** were isolated from the filtrate of the intermediate solution (Scheme 2). **CIPTIN** is stable when it is stored under ambient conditions and it is soluble in MeOH, CH_2Cl_2, DMSO and acetone.

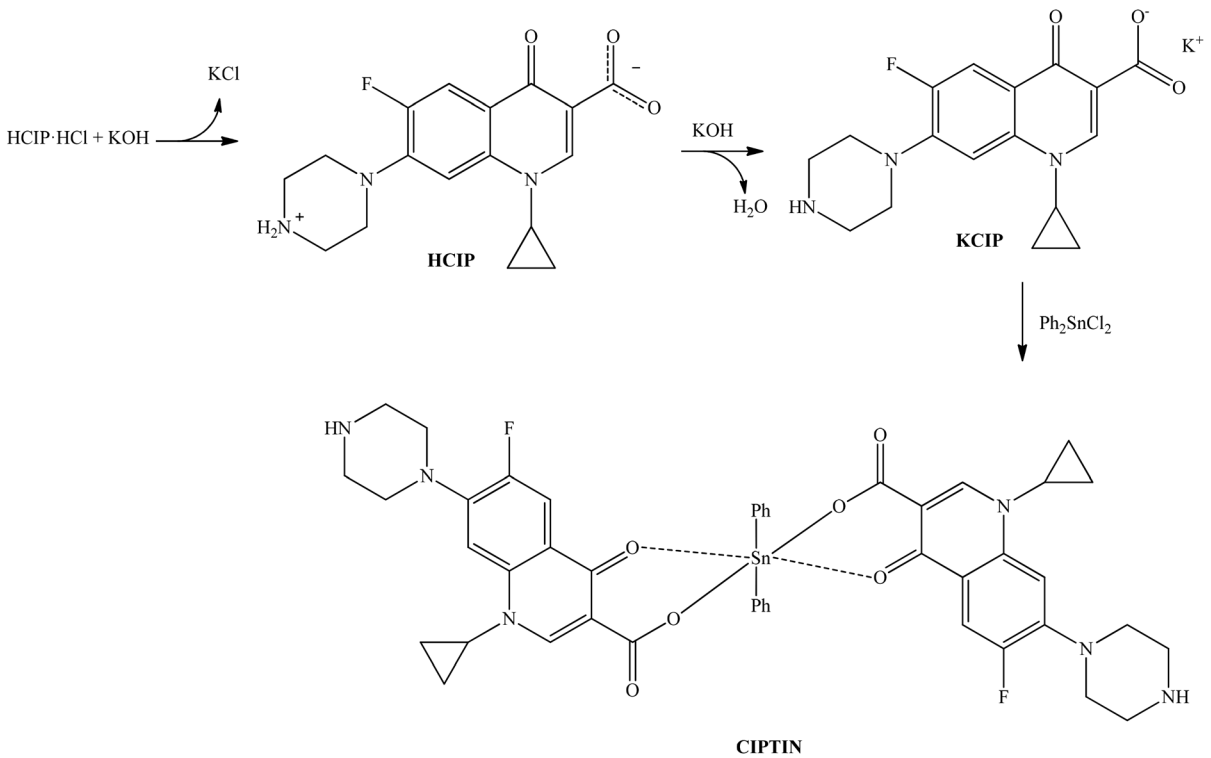

Scheme 2 Preparation reaction of **CIPTIN**.

Solid state studies

Crystal and molecular structure of CIPTIN and HCIP. Here, we report the crystal structures of the zwitterionic form of **HCIP** (anhydrous) and that of **CIPTIN** using single crystal X-ray crystallography for the first time. Unit cell parameters (only) of anhydrous **HCIP** were determined earlier using the powder X-ray diffraction data reported by Fabbiani *et al.*[18] The reported unit cell parameters reveal that **HCIP** crystallizes in the $P\bar{1}$

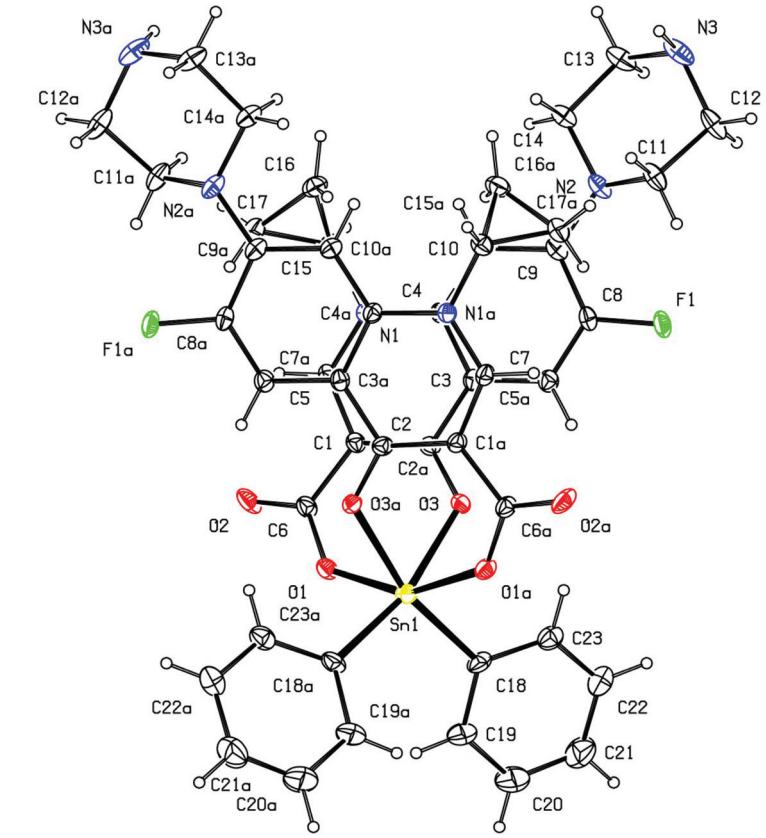

(A)

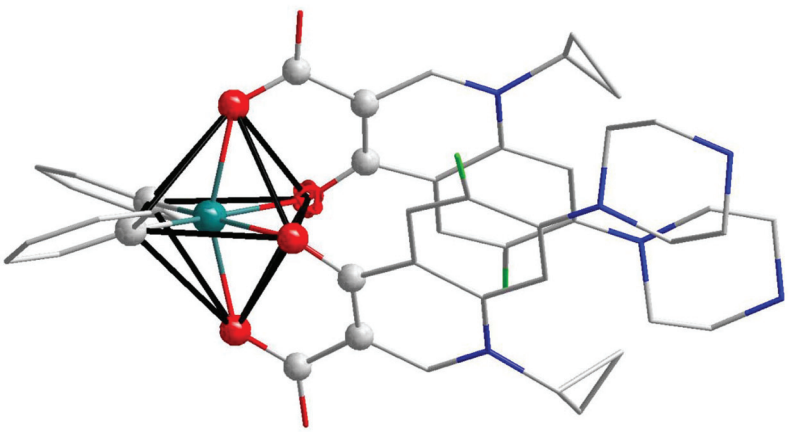

(B)

Fig. 1 (A) Molecular diagram together with the numbering scheme of **CIPTIN**. Selected bond lengths (Å) and angles [°]: Sn1–O1 = 2.135(3), Sn1–O3 = 2.158(3), Sn1–C18 = 2.120(5), Sn1–O1_a = 2.135(3), Sn1–O3_a = 2.158(3), Sn1–C18_a = 2.120(5), O3–C2 = 1.284(5), O1–C6 = 1.298(5), O2–C6 = 1.216(5), O1–Sn1–O3 = 79.93(11), O1–Sn1–O1_a = 155.64(11), O1–Sn1–O3_a = 81.60(11), O1_a–Sn1–O3 = 81.60(11), O3–Sn1–O3_a = 80.96(11), O1_a–Sn1–O3_a = 79.93(11). (B) The Δ-*cis*-[$Ph_2Sn(CIP)_2$] stereoisomer.

space group with a = 7.9606(2), b = 8.5798(2) and c = 10.7739(3) Å, α = 87.868(4), β = 87.868(4), γ = 88.212(4)°, V = 732.43(4) Å^3.[18] In our study, we found that **HCIP** (anhydrous) crystallizes in the $P\bar{1}$ space group with almost identical unit cell parameters: a = 7.8945(7), b = 8.5010(8) and c = 10.7522(9) Å and α = 87.440(7), β = 84.496(7), γ = 88.912(7)°, V = 717.47 Å^3. Since the synthesis of **CIPTIN** requires **HCIP HCl** as the starting material, **HCIP** is an intermediate of the methodology for the preparation. For this reason, a complete refinement of the crystal structure of **HCIP** was attempted independently to clarify the route followed. ORTEP diagrams of **CIPTIN** and **HCIP** along with their selected bond distances and angles are shown in Fig. 1 and 2.

CIPTIN is a covalent organotin compound. It consists of two ciprofloxacin ligands and one Ph_2Sn(IV) moiety. Ciprofloxacin coordinates to tin(IV) through the anionic oxygen atom of its deprotonated carboxylic group and the oxygen atom of its keto group. Thus, two oxygen atoms from each ciprofloxacin and two carbon atoms from the phenyl groups form a distorted octahedral (Oh) arrangement around the Sn(IV) ion. The equatorial plane of the octahedron around the Sn(IV) ion is constituted by two keto oxygen atoms (O3 and O3a) and two carbon atoms of phenyl groups (O3–Sn1–O3a = 80.96(11)° and O3–Sn1–C18a = 166.12(15)°). The axial positions are occupied by the two carboxylic oxygen atoms (O1 and O1a) (O1–Sn1–O1a = 155.64(11)°). The final arrangement of the ligands in **CIPTIN** lead to the Δ-*cis*-[$Ph_2Sn(CIP)_2$] stereoisomer (Fig. 1B). Only the Δ-*cis*-[$Ph_2Sn(CIP)_2$] isomer has been isolated in the crystal lattice indicating stereo-selectivity of the preparation reaction (Fig. 1B).

The two C–O bond distances of the carboxylic group (O1–C6 = 1.298(5) and O2–C6 = 1.216(5) Å) are almost equivalent, in **CIPTIN**, confirming deprotonation which it undergoes. The O1–C6 bond is slightly longer than the corresponding O2–C6 bond due to the donation of the O1 atom towards Sn(IV). The

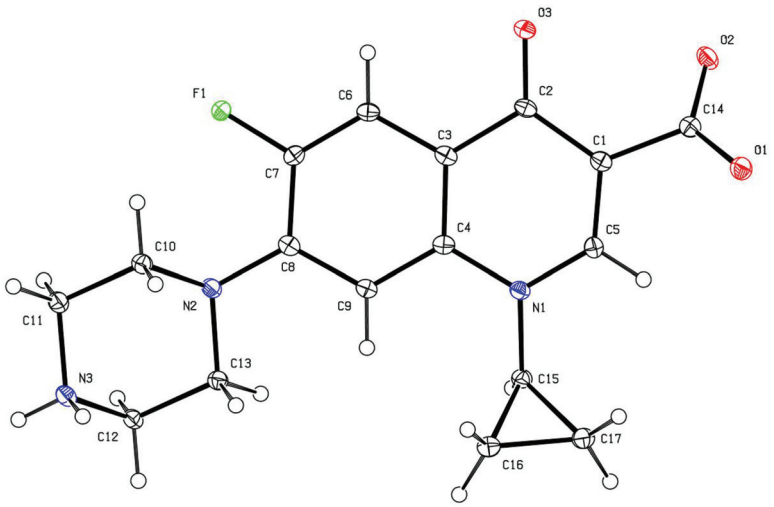

(A)

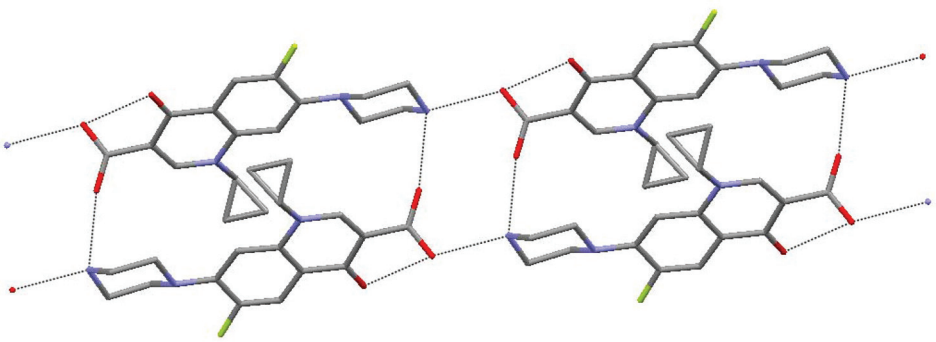

(B)

Fig. 2 (A) Molecular diagram together with the numbering scheme of **HCIP**. Selected bond lengths (Å) and angles [°]: O1–C14 = 1.247(3), O2–C14 = 1.266(3), C1–C2 = 1.453(3), O3–C2 = 1.241(3), N3–C11 = 1.481(3), N3–C12 = 1.485(3), O1–C14–O2 = 125.3(2), O3–C2–C1 = 125.0(2), C11–N3–C12 = 109.0(2). (B) 1D ribbon assembly established using hydrogen bonds.

C–O bond length of the keto group (O3–C2 = 1.284(5) Å) suggests the retention of the double nature of this bond.

The Sn–O bond distances (Sn1–O1 = 2.135(3) and Sn1–O3 = 2.158(3) Å) are in accordance with the corresponding distances found previously in [(*n*-Bu-)$_2$Sn(nap)$_2$] (napH = naproxen) (Sn1–O1 = 2.136(7) and Sn1–O2 = 2.506(6) Å),[19] in [Me$_2$Sn(salH)$_2$] (salH$_2$ = salicylic acid) (Sn1–O171 = 2.1069(18), Sn1–O271 = 2.1087(15), Sn1–O172 = 2.5145(15) and Sn1–O272 = 2.5773(15) Å)[20] and in [(*n*-Bu)$_2$Sn(salH)$_2$] (Sn1–O172 = 2.121(3), Sn1–O272 = 2.105(4), Sn1–O171 = 2.565(4) and Sn1–O271 = 2.632(4) Å).[20] However, in the cases of [(*n*-Bu-)$_2$Sn(nap)$_2$], [Me$_2$Sn(salH)$_2$] and [(*n*-Bu)$_2$Sn(salH)$_2$], the ligands chelate to Sn(IV), through their carboxylic groups.

Strong hydrogen bonding interactions N3[H3]···O2 = 2.733 (6) Å lead to 2D layers (Fig. 3). The layers consist of squares which are formed by four **CIPTIN** molecules (Sn···Sn = 13.969 Å and Sn–Sn–Sn = 87.03°).

The two C–O bond distances of the carboxylic group in anhydrous **HCIP** (O1–C14 = 1.247(3) and O2–C14 (1.266(3) Å) are equivalent suggesting its de-protonation (Fig. 2). The corresponding C1–O1 and C1–O2 bond lengths of the HCIP hexahydrate (**HCIP·6H$_2$O**) are 1.259(2) and 1.255(2) Å respectively.[8] Moreover, the O1–C14–O2 angle is 125.3(2)°. This is in accordance with the corresponding bond angle found in **HCIP·6H$_2$O** (125.11(12)°).[8] The N3–C11 and N3–C12 bond distances, on the other hand, are 1.481(3) and 1.485(3) Å, respectively, suggesting single N–C bonds (Fig. 2). This is further supported by the C11–N3–C12 bond angle of 109.0(2)°, which is close to the ideal 108°28′ of the sp^3 hybrid. Given the fact that two hydrogen atoms bind to N3, a positive charge is assumed for the ([–NH$_2$–])$^+$ group. Therefore, the charge distribution of the zwitterionic anhydrous **HCIP** is shown in Scheme 2.

Hydrogen bonds N3[H3]···O2 = 2.623(3) Å and N3[H3]···O1 = 2.882(3) Å lead to the 1D ribbon assembly (Fig. 2B).

Vibrational spectroscopy. The characteristic vibration bands of the free ligand (**HCIP·HCl**) at 1710 cm^{-1}, 1620 cm^{-1} and 1385 cm^{-1} are assigned to the C=O, ν_{asym}(COO) and ν_{sym}(COO) vibrations, respectively (Fig. S1†). The absence of the vibration band at 1710 cm^{-1} in the spectrum of **CIPTIN** suggests the coordination of the ligand through the oxygen atom of the keto C=O group (Fig. S1†). The ν_{asym}(COO) and ν_{sym}(COO) vibration bands are shifted at 1622 cm^{-1} and 1381 cm^{-1}, respectively in the spectrum of **CIPTIN**. The presence of the C=N bond of **CIPTIN** at 1272 cm^{-1} suggests that this N atom is not involved in the coordination sphere of the metal. The absence of the (O–H) vibration at 3520 cm^{-1} in the

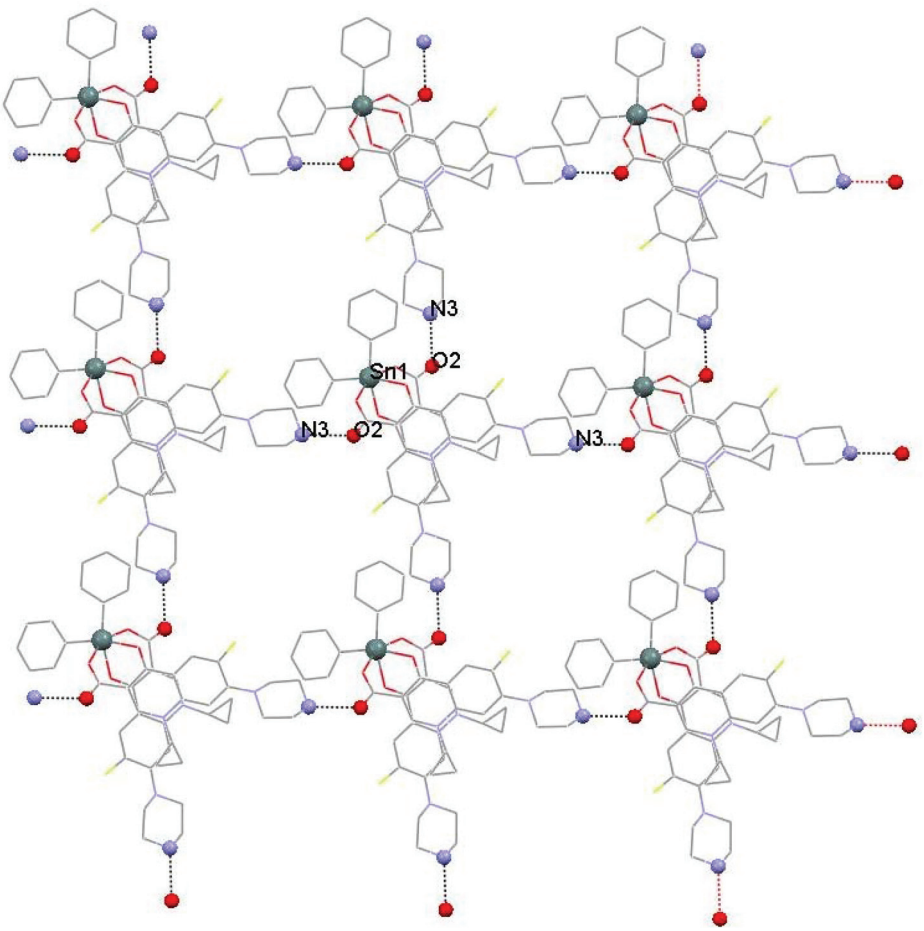

Fig. 3 Strong hydrogen bonding interactions O2[H2]···N3 lead to the 2D layer architecture.

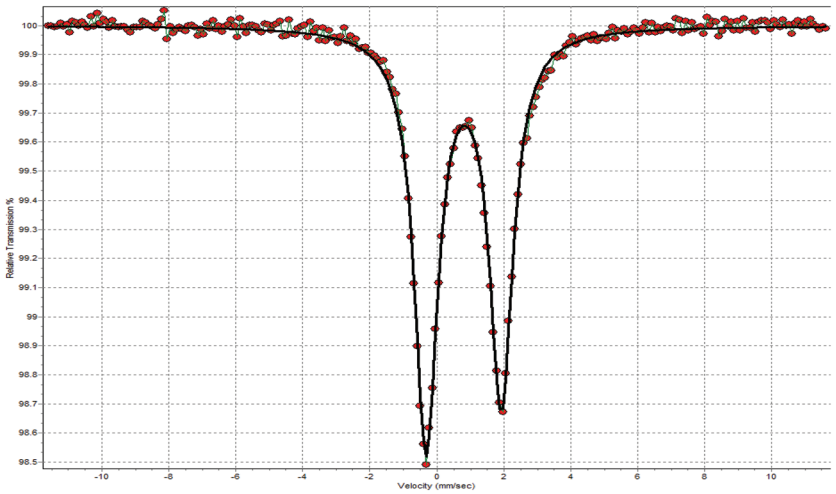

Fig. 4 The ^{119}Sn Mössbauer spectrum of **CIPTIN** at 77 K.

CIPTIN spectrum indicates the deprotonation of the carboxyl group. Therefore, ciprofloxacin is coordinated to the tin metal ion *via* the keto and carboxyl oxygen atom (Fig. S1†).

X-ray powder diffraction (XRPD) analysis. The XRPD spectrum of the powder of **CIPTIN** is identical to the simulated one which is derived by using single crystal XRD data (Fig. S2†). This indicates that the formula of the molecular structure of **CIPTIN** remains unchanged throughout the sample.

^{119}Sn Mössbauer spectroscopy. The ^{119}Sn Mössbauer spectrum at 77 K of **CIPTIN** is shown in Fig. 4. The spectrum of **CIPTIN** consists of one asymmetric Lorentzian doublet. The occurrence of one Lorentzian doublet indicates either the existence of one type of Sn atom in **CIPTIN** or one structural isomer.[11,21,22] The value of the Isomer Shift (I.S.) of **CIPTIN** is +0.804 mm s^{-1} which corresponds to the (4+) oxidation state.[11,21,22] The I.S. of the R_2Sn(IV) species lies between +0.737 and +1.777 mm s^{-1}.[11,21,22] The quadrupole splitting parameter (ΔE_q) value is 2.242 mm s^{-1}. Therefore, the *cis*-octahedral geometry should be concluded for the tin(IV) ion in the case of **CIPTIN**, since the ΔE_q value lies between 1.3 and 2.5 mm s^{-1}.[11,21,22] This value indicates an octahedral geometry with *cis*-R_2Sn(IV) (R = alkyl), around the tin atom of **CIPTIN** in accordance with the X-ray structure.

X-ray fluorescence (XRF) spectroscopy. The content of **CIPTIN** in Sn is 15.5 ± 2.3 wt%, while that calculated for $C_{46}H_{44}F_2N_6O_6Sn$ is 12.75%.

Thermal analysis. The TG-DTA analysis of **CIPTIN** shows decomposition within 6 steps (112.6–617.4 °C) with a total mass loss of 57.92% (Fig. S3†). The remaining 42.08% is due to $[(SnO_2)_2]$ (which corresponds to Sn: 13.68%; calc for $C_{46}H_{44}F_2N_6O_6Sn$: 12.75%).

Solution studies

Stability studies. The stability of **CIPTIN** was tested in DMSO and DMSO/water solutions by UV spectroscopy (Fig. S4 and S5†) and ^{1}H NMR for a period of 96 h (Fig. S6†). This period was chosen for stability testing, since the biological experiments require 24 or 48 h of incubation with **CIPTIN**. No changes were observed between the initial UV or ^{1}H NMR spectra and the corresponding spectra after 96 h, confirming the retention of **CIPTIN** in solution (Fig. S4–S6†).

^{1}H NMR studies. A broad resonance signal in the ^{1}H NMR spectrum of **HCIP·HCl** at 9.45 ppm is attributed to H [$N_{piperazine\ ring}$][8] (Fig. S7†). This signal is shifted at 8.87 ppm in **CIPTIN**. The resonance signals at 8.68, 7.97–7.92, and 7.62–7.59 ppm in the spectrum of **HCIP·HCl** are assigned to H [^{2}C], H[^{5}C] and H[^{8}C], respectively (Scheme 1).[8] These signals are observed at 8.67, 7.95–7.92, and 7.79–7.81 ppm in the spectrum of **CIPTIN**. The resonance signals of H[^{a}C], H[^{b}C], and cyclopropyl (–CH_2–) in the spectrum of **HCIP·HCl** appeared at 3.85, 3.47, and 1.33–1.19 ppm, respectively.[8] These signals undergo no shift in the case of **CIPTIN**. The resonance signals of **DPTD** at 8.05–7.80 and 7.42–7.28 ppm are shifted in the spectrum of **CIPTIN** at 7.72–7.58 and 7.31–7.16 ppm, respectively, indicating the coordination of tin to the antibiotic. Moreover, the resonance signal in the spectrum of **CIPTIN**, at 3.16 ppm is attributed to methanol, which was used as a solvent for the synthesis reaction.

Electrospray ionisation mass spectrometry (ESI-MS). In order to confirm the retention of the formula of **CIPTIN** in methanol solution, its ESI-MS spectrum was recorded. The ESI-MS spectrum of **CIPTIN** is dominated by the fragment at *m*/*z* 600.0–609.0, which is attributed to $[Ph_2Sn(CIP)]^+$ (calculated for $[C_{29}H_{27}N_3O_3FSn]^+$: *m*/*z*: 599.1 to 609.1) (Fig. S8†). The presence of this species which is derived from **CIPTIN** by cleavage of the one Sn–C(Ph) bond as part of the decomposition pattern of $[Ph_2Sn(CIP)_2\text{-}H^+]$ assumes the existence of **CIPTIN** in the solution, initially.

Antimicrobial studies

Minimum inhibitory concentration (MIC). The Gram-negative (*P. aeruginosa* and *E. coli*) and Gram-positive (*S. aureus* and *S. epidermidis*) bacteria are among the most concerning pathogens in humans involved in antibiotic resistance.[23,24] The anti-

microbial ability of **CIPTIN** towards these strains was evaluated, in terms of MIC values. The MIC is defined as the lowest concentration for the bacterial growth inhibition.[8–10,14–17]

The broth dilution method was used for the determination of the MIC values of **CIPTIN**, **HCIP·HCl**, **HCIP** and **DPTD**, upon incubation of Gram-negative (*P. aeruginosa* and *E. coli*) or Gram-positive (*S. aureus* and *S. epidermidis*) bacteria for 20 h (Table 1).

The MIC values of **CIPTIN** lie in the range of nanomolar concentrations against *P. aeruginosa*, *E. coli*, *S. aureus* and *S. epidermidis*, (0.741 ± 0.035, 0.301 ± 0.062, 1.179 ± 0.083 and 0.255 ± 0.041 μM, respectively) (Table 1, Fig. S9†). The corresponding MIC values of the drug in **HCIP·HCl** and **HCIP** are: 1.174 ± 0.221 μM and 1.048 ± 0.037 μM (*P. aeruginosa*), 0.938 ± 0.347 μM and 0.443 ± 0.041 μM (*E. coli*), 1.454 ± 0.123 μM and 1.459 ± 0.013 μM (*S. aureus*) and 1.079 ± 0.121 μM and 0.699 ± 0.025 μM (*S. epidermidis*), respectively (Fig. S10 and S11†).[8] The MIC values of **DPTD**, on the other hand, lie in the micromolar range of concentrations for the tested bacteria: >100 μM, 25.713 ± 1.535 μM, 47.529 ± 8.761 μM and 13.743 ± 0.263 μM towards *P. aeruginosa*, *E. coli*, *S. aureus* and *S. epidermidis*, respectively (Fig. S12†). Thus, **CIPTIN** shows 1.2 to 4.2-fold stronger antimicrobial activity than those of **HCIP·HCl** or **HCIP** towards both Gram negative and positive bacteria. The strongest antimicrobial effect of **CIPTIN** is observed towards *S. epidermidis*, which is 4.2-fold higher than that of **HCIP·HCl** and 2.7-fold higher than that of **HCIP**. Moreover, **CIPTIN** activity rises up to 135-fold stronger than **DPTD** activity against these bacteria. Therefore, **CIPTIN** exhibits superior activity to that of both its ingredients (antibiotic and **DPTD**).

Microbes are classified into susceptible (MIC <50 μM) or resistant (MIC >100 μM) towards an antimicrobial agent by their MIC values.[8,10] Thus, all tested strains here are considered as susceptible to **CIPTIN**.

Minimum bactericidal concentration (MBC). The MBC values of **CIPTIN** were also evaluated. MBC is defined as the lowest concentration of an antibacterial agent that kills 99.9% of the initial bacterial inoculums.[8,10,14–17]

Table 1 MIC and MBC values and inhibition zones of **CIPTIN**, **CIPAG**, **PenAg**, **HCIP·HCl**, **HCIP**, **DPTD** and $AgNO_3$ against *P. aeruginosa*, *E. coli*, *S. aureus* and *S. epidermidis*

Compound	*P. aeruginosa*	*E. coli*	*S. aureus*	*S. epidermidis*	Ref.
MIC (μM)					
$Ph_2Sn(CIP)_2$ CIPTIN	0.741 ± 0.035	0.301 ± 0.062	1.179 ± 0.083	0.255 ± 0.041	[a]
Me_3SnCIP	0.253	1.012	0.125	—	13
Cy_3SnCIP	0.089	1.432	0.179	—	13
$Ag(CIP)_2NO_3$ CIPAG	0.612 ± 0.142	—	0.537 ± 0.067	0.458 ± 0.083	8
$[Ag(Pen)(DMSO)]_2$ PenAg	23.0 ± 2.290	—	0.080 ± 0.020	2.410 ± 0.880	9
HCIP·HCl	1.174 ± 0.221	0.938 ± 0.347	1.454 ± 0.123	1.079 ± 0.121	8
HCIP	1.048 ± 0.037	0.443 ± 0.041	1.459 ± 0.013	0.699 ± 0.025	[a]
PenNa	>2000	—	0.140 ± 0.020	3.760 ± 1.140	9
Ph_2SnCl_2 DPTD	> 100	25.713 ± 1.535	47.529 ± 8.761	13.743 ± 0.263	[a]
$AgNO_3$	60.0	—	79.500	39.400	8
MBC (μM)					
$Ph_2Sn(CIP)_2$ CIPTIN	0.800 ± 0.195	0.445 ± 0.040	1.600 ± 0.110	0.667 ± 0.045	[a]
Me_3SnCIP	0.506	1.012	0.506	—	13
Cy_3SnCIP	0.716	2.863	0.358	—	13
$Ag(CIP)_2NO_3$ CIPAG	0.700	—	1.000	0.800	8
$[Ag(Pen)(DMSO)]_2$ PenAg	46.6	—	—	—	9
HCIP·HCl	1.6	1.624 ± 0.127	2.000	1.600	8
HCIP	1.280 ± 0.096	1.250 ± 0.098	2.225 ± 0.050	1.200 ± 0.160	[a]
PenNa	2000	—	—	—	9
Ph_2SnCl_2 DPTD	> 100	> 100	> 100	> 100	[a]
$AgNO_3$	91.5		95.0	140.0	8
MBC/MIC					
$Ph_2Sn(CIP)_2$ CIPTIN	1.08	1.48	1.36	2.62	[a]
Me_3SnCIP	2.0	1.0	4.05	—	13
Cy_3SnCIP	8.04	2.0	2.0	—	13
$Ag(CIP)_2NO_3$ CIPAG	1.14	—	1.86	1.75	8
HCIP·HCl	1.36	1.73	1.38	1.48	8
HCIP	1.22	2.82	1.53	1.72	[a]
$AgNO_3$	1.53		1.19	3.55	8
IZ (mm)					
$Ph_2Sn(CIP)_2$ CIPTIN	40.8 ± 1.5	34.0 ± 0.8	36.0 ± 1.1	42.7 ± 0.8	[a]
$Ag(CIP)_2NO_3$ CIPAG	32	—	28	34	8
$[Ag(Pen)(DMSO)]_2$ PenAg	17	—	57	34	9
HCIP·HCl	32.0	32.0 ± 0.8	24.0	36.0	8
HCIP	35.5 ± 0.6	33.0 ± 0.8	30.5 ± 0.6	39.2 ± 0.9	[a]
PenNa	10	—	60	34	9
Ph_2SnCl_2 DPTD	10.0± 0.0	18.7 ± 0.9	13.1 ± 0.6	15.8± 0.4	[a]
$AgNO_3$	13		12	14	8

[a] This study, **PenNa** = sodium salt of penicillin.

The MBC values of **CIPTIN** for Gram negative bacteria *P. aeruginosa* and *E. coli* are 0.800 ± 0.195 μM and 0.445 ± 0.040 μM respectively, and against Gram positive bacteria *S. aureus* and *S. epidermidis* are 1.600 ± 0.110 μM and 0.667 ± 0.045 μM, respectively (Table 1, Fig. S13†). The corresponding MBC values of **HCIP·HCl** and **HCIP** are 1.200–2.225 μM against both Gram negative and Gram positive bacteria (Table 1, Fig. S14 and S15†). In the case of **DPTD**, the MBC values are higher than 100 μM (Fig. S16†). Thus, **CIPTIN** exhibits higher bactericidal activity than those of free drugs which rises up to 3.6-fold in respect of **HCIP·HCl** or up to 2.8-fold for **HCIP**. **DPTD** has no bactericidal activity.

Since the MBC/MIC values of **CIPTIN** lie between 1.08 and 2.62, against the tested microbial strains, (Table 1) **CIPTIN** is classified into bactericidal agents. This is because when the MBC/MIC value is ≤2, an agent is considered as a bactericidal agent, while when the MBC/MIC value is ≥4, as a bacteriostatic agent.[8,10,14–17] The MBC/MIC values of **HCIP·HCl** and **HCIP** varied between 1.22 and 2.82 and they are bactericidal drugs.

Inhibition zone (IZ). The IZ was evaluated with the agar disk-diffusion method.[8,10,14–17] The calculated diameter of the IZ is used to determine the effectiveness of an antibiotic. Therefore, the bacterial strains might be classified as susceptible to an agent based on the IZ developed.[8,10,14–17] Thus, Shungu *et al.*[25] classified the microbes into three categories according to the size of the IZ caused by antibiotics. (i) Those strains where the antibiotic causes IZ ≥17 mm and they are consider as susceptible, (ii) those where the antibiotic creates the IZ between 13 and 16 mm (13 ≤ IZ ≤ 16 mm) are intermediate, (iii) those where the antibiotic causes the IZ ≤12 mm, and they are considered as resistant strains.[25]

The IZs caused by **CIPTIN** determined against *P. aeruginosa*, *E. coli*, *S. aureus* and *S. epidermidis* are 40.8 ± 1.5, 34.0 ± 0.8, 36.0 ± 1.1 and 42.7 ± 0.8 mm, respectively classifying these strains into susceptible ones towards **CIPTIN** (Fig. 5). The ranges of IZs, which were caused by **HCIP·HCl** and **HCIP**, lie between 32.0 and 35.5 mm (against Gram negative bacteria) and 24.0–39.2 mm (against Gram positive bacteria). These values classify the tested bacteria into susceptible ones against **HCIP·HCl** and **HCIP** (Table 1, Fig. S17†). The corresponding IZs developed by **DPTD** lie between 10.0 and 18.7 mm against the tested bacteria classifying them into resistant or intermediate ones towards **DPTD**. Generally, **CIPTIN** causes greater inhibition zones than those of the commercial antibiotic or **DPTD**, against both negative and positive bacterial strains.

Effect on biofilm formation by CIPTIN. The effect of **CIPTIN** on biofilm eradication was tested against biofilm-positive strains (*P. aeruginosa* and *S. aureus*) by the Biofilm Elimination Concentration (BEC) values with crystal violet assay.[8–10,14–17] The BEC is the required concentration to reduce the viability of biofilm bacteria by 99.9%, at least.[8–10,14–17] The BEC value of **CIPTIN** for *P. aeruginosa* is 656 μM and for *S. aureus* is 752 μM

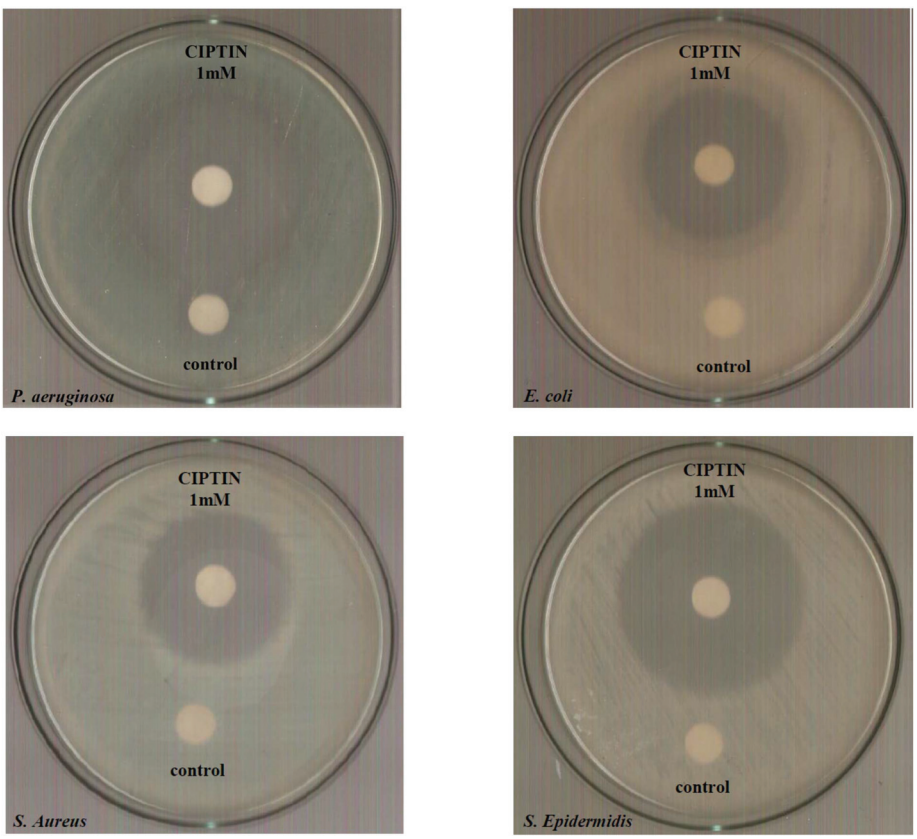

Fig. 5 Inhibition zones of **CIPTIN** against *P. aeruginosa* (A), *E. coli* (B), *S. aureus* (C) and *S. epidermidis* (D).

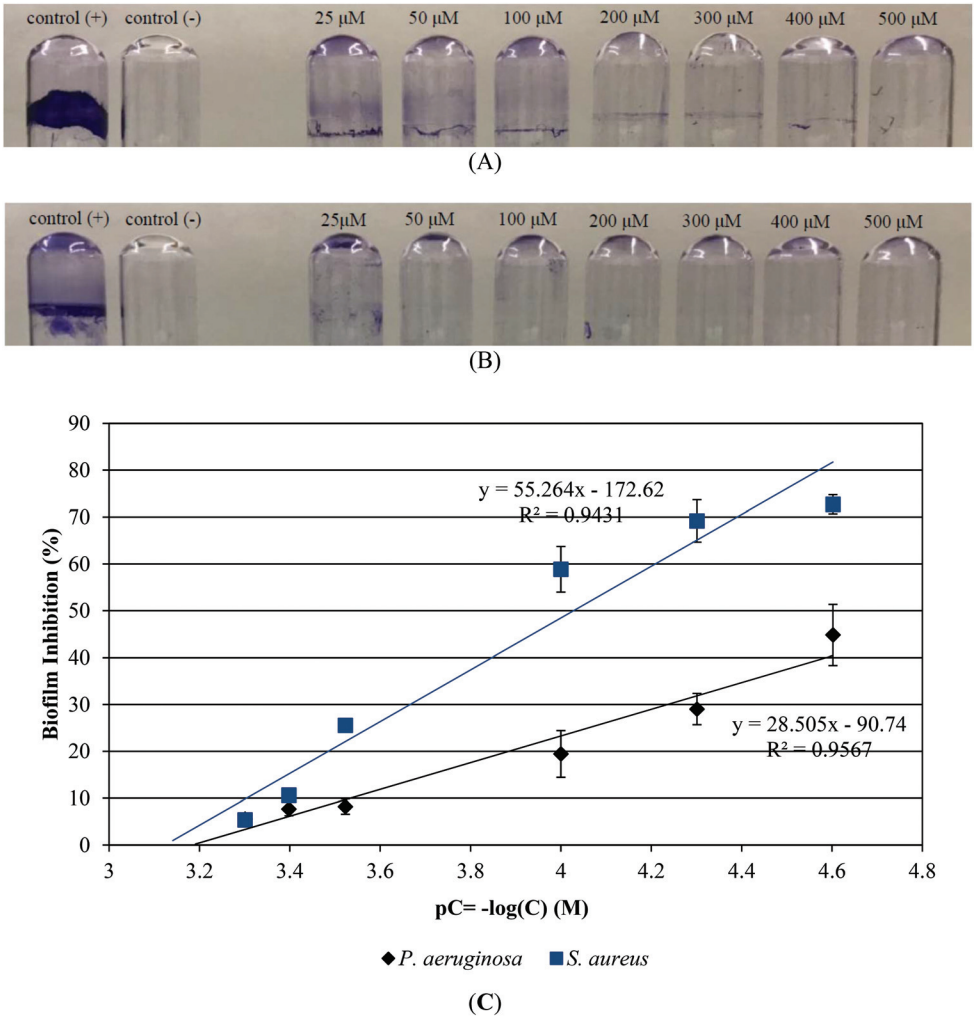

Fig. 6 Crystal violet staining revealing biofilm of *P. aeruginosa* (A) and *S. aureus* (B) with increasing concentrations of **CIPTIN**. Biofilm inhibition (%) of *P. aeruginosa* and *S. aureus versus* pC = −log(C) (M) of **CIPTIN** (C).

(Fig. 6). We have recently determined the BEC value of **HCIP·HCl** against *P. aeruginosa* (670 μM) and *S. aureus* (952 μM).[8] The corresponding BEC values of **HCIP** are: 2140 μM (*P. aeruginosa*) and 2463 μM (*S. aureus*) (Fig. S19†). **CIPTIN** eliminates the biofilm of *P. aeruginosa* and *S. aureus* more efficiently than the neutral drug **HCIP**, while its BEC value is comparable with the corresponding value of **HCIP·HCl**.

Evaluation of the *in vitro* toxicity of CIPTIN. Immortalized human keratinocyte (HaCaT) cells were used to test the *in vitro* cytotoxic effect of **CIPTIN**, **HCIP·HCl**, **HCIP** and **DPTD**, by sulforhodamine B (SRB) assay, upon their incubation with the agents by 48 h. The IC_{50} value of **CIPTIN** is 2.33 ± 0.2 μM. The corresponding IC_{50} values of **HCIP·HCl** and **HCIP** are >30 μM, while that of **DPTD** is 1.09 ± 0.1 μM.

The therapeutic window of an agent is defined by the selectivity index (SI):[8,26]

$$SI = IC_{50(\text{against HaCaT cells})}/MIC_{(\text{against tested bacteria})}$$

The higher the SI, the greater the antimicrobial effect and the lower the cellular toxicity. The SI values of **CIPTIN** are 3.1 (*P. aeruginosa*), 7.7 (*E. coli*), 2.0 (*S. aureus*) and 9.1 (*S. epidermidis*). These values constitute a wide therapeutic window for **CIPTIN**. The SI values of **DPTD** are: >0.01, 0.04, 0.02 and 0.08 against *P. aeruginosa*, *E. coli*, *S. aureus* and *S. epidermidis* respectively.

Evaluation of *in vitro* genotoxicity by micronucleus assay. The micronucleus assay is frequently used to evaluate the mutagenic, genotoxic or teratogenic effect of metallodrugs.[27] In the presence of a genotoxic factor, micronuclei (MN) appear as small membrane-bound DNA fragments in the cytoplasm of interphase cells and they are formed during the metaphase–anaphase transition of the mitotic cycle.[28] The micronucleus assay has been widely used in monitoring genetic damage in order to avoid the screening of drugs on animals.

In order to evaluate the genotoxicity of **CIPTIN**,·**HCIP·HCl**, **HCIP** and **DPTD**, HaCaT cells were treated using the agents at their IC_{50} values (Fig. 7). The corresponding frequency of micronucleus after treatment of HaCaT cells using **CIPTIN** is 2.60 ± 0.15%, while the frequency without treatment of the cells is 2.17 ± 0.05%. Therefore, **CIPTIN** exhibits negligible genotoxicity. The micronucleus frequencies of HaCaT cells

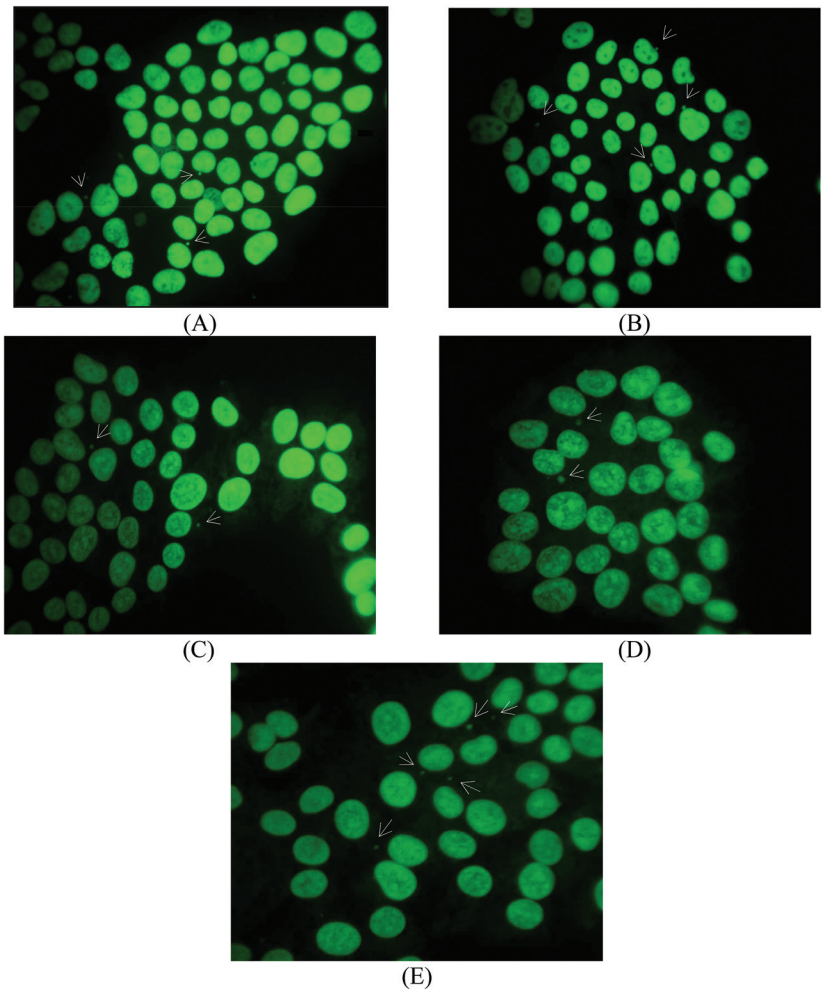

Fig. 7 Representative snapshots of micronucleus formed in untreated HaCaT cells (A) and upon their treatment with **CIPTIN** (B), **HCIP·HCl** (C), **HCIP** (D) or **DPTD** (E) at 2.33 μM for 48 h.

after treatment using **HCIP·HCl** (2.44 ± 0.2)% or **HCIP** (2.48 ± 0.1)% are close to that of **CIPTIN**. The MN formed upon treatment of HaCaT cells using **DPTD** is 3.05 ± 0.2%, which is significantly higher than that of **CIPTIN**.

Conclusions

The design and the development of antimicrobial agents are of great importance. The new metalloantibiotic **CIPTIN** has been synthesized and characterized within this work. The crystal structure reveals that the geometry around the metal center is octahedral (Fig. 1B). The stereoselective synthesis results in the Δ-*cis*-$[Ph_2Sn(CIP)_2]$ isomer only (Fig. 1B). 2D layer supramolecular assemblies are established based on strong hydrogen bonding interactions (Fig. 3). Four molecules form square planes with their tin atoms placed on the edges. These constitute the building blocks of the layers (Fig. 3). The area covered by each square is 195.133 $Å^2$.

CIPTIN has been evaluated towards the Gram negative microbes *P. aeruginosa* and *E. coli* and Gram positive microbes *S. aureus* and *S. epidermidis*. **CIPTIN** is classified as a bactericidal agent against *P. aeruginosa*, *E. coli*, *S. aureus* and *S. epidermidis* (Table 1), while these microbes are ranked among those susceptible to it (IZ values) (Table 1).

The antibacterial activity of **CIPTIN** (Δ-*cis*-$[Ph_2Sn(CIP)_2]$) is compared to that of **CIPAG** with the formula ({$[Ag(HCIP)_2]NO_3^{\bullet}$}),[8] $[Me_3Sn(CIP)]$, and $[Cy_3Sn(CIP)]$[13] and **PenAg** with the formula $[Ag(Pen)(CH_3OH)]_2$, (HPen = penicillin)[9] and their ingredients **HCIP·HCl**, **HCIP**, **PenNa**, **DPTD** and $AgNO_3$ (Table 1, Fig. 8).

CIPTIN exhibits stronger activity compared to ciprofloxacin against both the tested Gram positive and Gram negative bacteria as well as $[Me_3Sn(CIP)]$ and $[Cy_3Sn(CIP)]$,[13] suggesting that the presence of the tin(IV) ion enhances the effectiveness of ciprofloxacin even more (Table 1, Fig. 8). Although the activity of **DPTC** is significantly lower than that of **CIPTIN**, this should be attributed to the synergistic effect of both the organotin moiety and ciprofloxacin. **CIPTIN** exhibits superior activity to penicillin against Gram negative microbes, as expected since penicillin is inactive against Gram negative bacteria microbes (Fig. 8). Against Gram positive microbes,

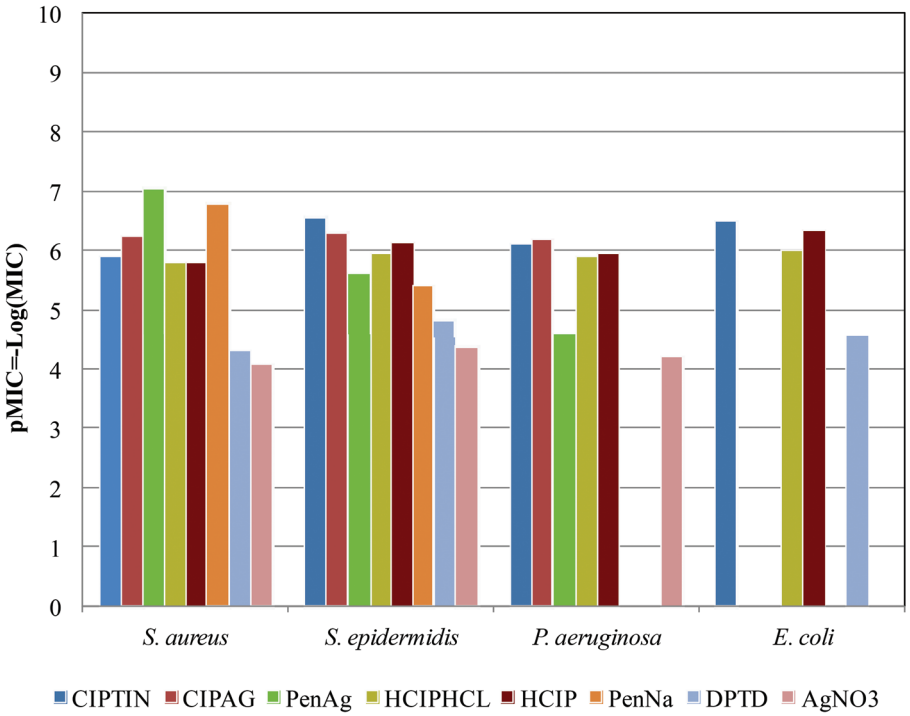

Fig. 8 Histogram of pMIC (–log(MIC)) values of **CIPTIN** (Δ-*cis*-[$Ph_2Sn(CIP)_2$]), ({[$Ag(HCIP)_2$]NO_3·}),[8] **PenAg** [$Ag(Pen)(CH_3OH)]_2$, (HPen = penicillin),[9] **HCIP·HCl**, **HCIP**, **PenNa**, **DPTD** and $AgNO_3$, against *S. aureus*, *S. epidermidis*, *P. aeruginosa* and *E. coli*.

CIPTIN exhibits stronger activity against *S. epidermidis*, while penicillin shows higher activity against *S. aureus* (Fig. 8). Given the fact that ciprofloxacin exhibits stronger activity than penicillin against *S. epidermidis*, while penicillin against *S. aureus*, **CIPTIN** follows the relative efficiency of ciprofloxacin towards penicillin. Among the compounds of ciprofloxacin, **CIPTIN** exhibits higher activity compared to **CIPAG** against *S. epidermidis*, which however is more effective against *S. aureus* and *P. aeruginosa* (Fig. 8). Therefore, the antibiotic activity is differentiated by the type of metal ion which coordinates with the drug. Moreover, among organotins, [$Me_3Sn(CIP)$] and [$Cy_3Sn(CIP)$][13] show stronger activity compared to **CIPTIN** against *P. aeruginosa* and *S. aureus* (Table 1). However, this should be assigned to the higher toxicity of tri-organotin moieties than to that of di-organotin moieties. Although **PenAg** shows better activity against *S. aureus*, **CIPTIN**, however is more drastic against *S. epidermidis* and *P. aeruginosa*, where ciprofloxacin itself shows better activity compared to free penicillin (Fig. 8). Therefore, the activity of the metallodrug follows the corresponding efficiency of the antibiotic, regardless of the type of metal ion Sn(IV) or Ag(I). Moreover, **CIPTIN** shows superior activity to that of silver(I) nitrate against all the tested microbes (Fig. 8), confirming that the conclusion is already drawn for the synergy of the metal ion with the drug on the activity of the metallodrug. **CIPTIN** eliminates the biofilm in a similar manner to that of the drug (Table 1). The *in vitro* toxicity of **CIPTIN** against HaCaT cells shows a selectivity index (SI) higher than 1 suggesting a wide therapeutic window, while its *in vitro* genotoxicity is even lower than that of **HCIP·HCl** or **HCIP**.

In conclusion, the coordination of a drug on a metal ion strongly enhances its activity. The antimicrobial information which has been stored in a drug affects the activity of the metallodrug and it is affected by the coordination demands stored in the metal ion, creating a combination of a new entity with enhanced and novel biological properties.

Experimental

Materials and instruments

All solvents used were of reagent grade. Tryptone tryptophan medium, beef extract powder, peptone bacteriological, and soy peptone were purchased from Biolife. Agar and yeast extract were purchased from Fluka Analytical. Sodium chloride, D (+)-glucose, and di potassium hydrogen phosphate trihydrate were purchased from Merck. Dulbecco's modified Eagle's medium, (DMEM), fetal bovine serum, glutamine and trypsin were purchased from Gibco, Glasgow, UK. Phosphate buffer saline (PBS) was purchased from Sigma-Aldrich. Melting points were measured in open tubes with Stuart Scientific apparatus and are uncorrected. IR spectra in the region of 4000–370 cm^{-1} were obtained using a Cary 670 FTIR spectrometer, Agilent Technologies. A UV-1600 PC series spectrophotometer of VWR was used to obtain electronic absorption spectra. The ^1H NMR spectra were recorded using a Bruker AC 250, 400 MHFT-NMR instrument in DMSO-d_6. ESI-MS spectra were recorded with an Agilent 1100/LC–MS system. ^{119}Sn Mössbauer spectra were recorded at various sample tempera-

tures (85 K), with a constant-acceleration spectrometer equipped with a $CaSnO_3$ source kept at room temperature. The calibration of the spectrometer was carried out with a ^{57}Co source and an Fe absorber at room temperature. The line widths were very close to the natural width (0.28 mm s^{-1}). The content of the tin samples was calculated to be approximately 4 mg Sn in the 2-cm^2 area of the sample holder. XRF measurements were carried out using an Am-241 radio isotopic source (exciting radiation 59.5 keV). Thermogravimetry–Differential Thermal Analysis (TG–DTA) of **CIPTIN** was carried out using Seiko SII TG/DTA 7200 apparatus under a N_2 flow (40 cm^3 min^{-1}) with a heating rate of 10 K min^{-1}.

Synthesis and crystallization of CIPTIN

A clear solution of 0.5 mmol ciprofloxacin hydrochloride (**HCIP·HCl**) (0.184 g) in dd water (8 mL) was treated with 0.75 mmol KOH (750 μL 1 N). A solution of 0.25 mmol diphenyltin dichloride (**DPTD**) (0.086 g) in methanol (3 mL) was added to the previous one under continuous stirring for 30 min and the resulting white precipitation was immediately filtered off. Crystals of **CIPTIN** suitable for X-ray analysis were grown from slow evaporation of the solution after one day.

CIPTIN: Yellowish crystal, melting point: > 300 °C; elemental analysis found: C: 59.55; H: 4.92; N: 9.23%; calculated for $C_{46}H_{44}N_6O_6F_2Sn$: C: 59.19; H: 4.75; N: 9.00%. IR (cm^{-1}), (KBr): 3906w, 2965w, 2698w, 2487w, 2111w, 1918w, 1604w, 1474w, 1265s, 1142s, 1025s, 944vs, 809s, 739vs, 628s, 446s; ^1H NMR (ppm) in DMSO-d_6: 8.87 (s, H[$N_{piperazine\ ring}$]), 8.67 (s, H[^2C]), 7.95–7.92 (d, H[^5C]), 7.79–7.81 (d, H[^8C]), 7.72–7.58 (m, Ph-), 7.31–7.16 (m, Ph-), 3.85 (s, H[^aC]), 3.47 (d, H[^cC]), 1.33 (m, cyclopropyl CH_2), 1.19 (m, cyclopropyl CH_2); UV-vis (DMSO): λ = 284 nm ($\log \varepsilon$ = 4.68), λ = 320 nm ($\log \varepsilon$ = 4.21), 331 nm, ($\log \varepsilon$ = 4.20).

X-ray structure determination

Intensity data of the crystals of **CIPTIN** and **HCIP** were collected using an Oxford Diffraction CCD instrument, using graphite monochromated Mo radiation (λ = 0.71073 Å). Cell parameters were determined by least-squares refinement of the diffraction data from 25 reflections. All data were corrected for Lorentz-polarization effects and absorption.[29] The structures were solved with direct methods with SHELXS97 [30] and refined by full-matrix least-squares procedures on F^2 with SHELXL97.[31] All non-hydrogen atoms were refined anisotropically, and hydrogen atoms were located at calculated positions and refined *via* the "riding model" with isotropic thermal parameters fixed at 1.2 (1.3 for CH_3 groups) times the U_{eq} value of the appropriate carrier atom.

CIPTIN: $C_{46}H_{44}N_6O_6F_2Sn$, MW = 933.612, monoclinic, space group *I*2/*a*, *a* = 14.7410(6), *b* = 20.2602(5), *c* = 18.8558(7) Å, α = 90, β = 111.400(4), γ = 90°, *V* = 5243.1(3) $Å^3$, *Z* = 4, *T* = 100 K, ρ (calc) = 1.183 g cm^{-3}, μ = 4.320 mm^{-1}, *F*(000) = 1912. 10 180 reflections measured, 4682 unique (R_{int} = 0.052). The final R_1 = 0.0523 (for 3818 reflections with $I > 2\sigma(I)$) and w$R(F2)$ = 0.1428 (all data) *S* = 0.99.

HCIP: $C_{17}H_{18}FN_3O_3$, MW = 331.34, triclinic, space group $P\bar{1}$, *a* = 7.8945(7), *b* = 8.5010(7), *c* = 10.7522(9) Å, α = 87.440(7), β = 84.496(7), γ = 88.912(7)°, *V* = 717.47(11) $Å^3$, *Z* = 2, *T* = 100 K, ρ (calc) = 1.534 g cm^{-3}, μ = 0.967 mm^{-1}, *F*(000) = 348. 4189 reflections measured, 2531 unique (R_{int} = 0.041). The final R_1 = 0.0511 (for 1996 reflections with $I > 2\sigma(I)$) and w$R(F2)$ = 0.1440 (all data) *S* = 1.07.

Crystallographic data (excluding structure factors) for the structure reported in this paper has been deposited with the Cambridge Crystallographic Data Centre as supplementary publication no. CCDC 1993746 (**CIPTIN**), CCDC 2002394 (**HCIP**).†

Biological tests

Bacterial strains. The strains used were: *Pseudomonas aeruginosa* (*P. aeruginosa*), *Escherichia coli Dh5a* (*E. coli*), *Staphylococcus aureus* (*S. aureus*) subsp. aureus (ATCC® 25923™) and *Staphylococcus epidermidis* (ATCC® 14990™).

Solvents used. The biological experiments for antibacterial studies were carried out in DMSO/broth solutions of **CIPTIN**, **HCIP** and **DPTD** and in H_2O/broth solutions for **HCIP·HCl**. The biological experiments for cell viability and for micronucleus assay were carried out in DMSO/DMEM solutions 0.0005–0.03% v/v DMSO in DMEM for the tested compounds. Stock solutions of **CIPTIN**, **HCIP·HCl**, **HCIP** and **DPTD** (0.01 M) in DMSO were freshly prepared and diluted in broth or cell culture medium to the desired concentration.

Minimum inhibitory concentration (MIC) testing. This study was performed according to standard procedures, as described previously.[8–10,14–17] Briefly, the bacterial strains were streaked onto trypticase soy agar plates, which were incubated for 18–24 h at 37 °C. Then, three to five isolated colonies were selected of the same morphological appearance from the fresh agar plate using a sterile loop and transferred into a tube containing 2 mL of sterile saline solution. The optical density at 620 nm is 0.1, which corresponds to 10^8 cfu per mL. The final inoculum size for broth dilution is 5×10^5 cfu per mL. The total volume of the culture solution treated with **CIPTIN**, **HCIP·HCl**, **HCIP** or **DPTD**, and the total volumes of the positive and negative controls, were 2 mL. The range of concentrations of **CIPTIN** was 100–1600 nM, of **HCIP·HCl** was 100–800 nM, of **CIPH** was 200–1600 nM and of **DPTD** was 5000–100 000 nM. The growth was assessed after incubation for 20 h. The MIC value was determined as the concentration of the compound which inhibits the visible growth of the bacterium being investigated, while it is confirmed by measuring the solution optical density at 620 nm *vs.* concentrations.[8–10,14–17]

Minimum bactericidal concentration testing. In order to determine MBC values of **CIPTIN**, the bacteria were initially cultivated in the presence of **CIPTIN**, **HCIP·HCl**, **HCIP** or **DPTD** in broth for 20 h. Afterwards, the MBC value was determined in duplicate, by subculturing 4 μL of the broth with bacteria and **CIPTIN**, **HCIP·HCl**, **HCIP** or **DPTD** in an agar plate. Bactericidal activity occurs when no colony formation is observed. The lowest concentration at which the tested compounds could give complete inhibition of the growth of microbes was defined as the MBC value.[8–10,14–17]

Determination of the inhibition zone (IZ) through the agar disk-diffusion method. As described previously,[8–10,14–17] agar plates were inoculated with a standardized inoculum (10^8 cfu per mL) of the tested microorganism. Filter paper disks (9 mm in diameter), which had been previously soaked with **CIPTIN**, **HCIP·HCl**, **HCIP** or **DPTD** (10^{-3} M), were placed on the agar surface. The Petri dishes were incubated for 20 h, and then the diameters of the inhibition zones were measured.

Effects on biofilm formation. Bacterial strains of *P. aeruginosa* or *S. aureus* with a density of 6.7×10^6 cfu per mL were inoculated into LB medium (total volume = 1500 μL) and cultured for 24 h at 37 °C. Afterwards, the content of each tube was carefully removed and the tubes were washed with 1 mL of dH_2O. The negative control contained broth only. Then, the bacteria were incubated with **CIPTIN** at concentrations between 25 and 500 μM (total volume = 2000 μL) for 20 h, at 37 °C. The content of each tube was aspirated, each tube was washed three times with 1 mL of methanol and 2 mL of ddH_2O and left to dry. Then, the tubes were stained for 15 min with crystal violet solution (0.1% w/v). Excess stain was rinsed off with 1 mL of methanol and 2 mL of ddH_2O. The tubes were left to dry for 24 h and the bounded crystal violet was released by adding 30% glacial acetic acid (2 mL) and after 3 mL of ddH_2O. The optical density of the solution yielded is measured at 550 nm, to give the biofilm biomass.[8–10,14–17]

In vitro toxicity evaluation

Sulforhodamine B assay. These studies were performed in accordance with the previously reported method.[10,15] Briefly, HaCaT cells were seeded in a 96-well plate in a density of 8000 cells and after 24 h of cell incubation, the compounds were added in the concentration range of 0.25–3 μM (for **CIPTIN** and **DPTD**) and 0.5–30 μM (for **HCIP·HCl** and **HCIP**). After 48 h of incubation of HaCaT cells with the compounds, the culture medium was aspirated and the cells were fixed with 50 μL of 10% cold trichloroacetic acid (TCA). The plate was left for 30 min at 4 °C, washed five times with deionized water, and left to dry at room temperature for at least 24 h. Subsequently, 70 μL of 0.4% (w/v) sulforhodamine B (Sigma) in 1% acetic acid solution was added to each well and left at room temperature for 20 min. SRB was removed, and the plate was washed five times with 1% acetic acid before air drying. Bound SRB was solubilised with 200 μL of 10 mM un-buffered Tris-base solution. Absorbance was read using a 96-well plate reader at 540 nm.

Evaluation of genotoxicity by micronucleus assay. The micronucleus assay was carried out as previously described.[27] Briefly, HaCaT cells were seeded (at a density of 240 000 cells per well) in glass cover slips which were afterwards placed in six-well plates, with 3 mL of cell culture medium and incubated for 24 h. HaCaT cells were exposed with compounds in IC_{50} values for a period of 48 h. The number of micronucleated cells per 1000 cells was determined.

Conflicts of interest

There are no conflicts to declare.

Acknowledgements

[i] This research has been co-financed by the European Union and Greek national funds through the Operational Program Competitiveness, Entrepreneurship and Innovation, under the call RESEARCH – CREATE – INNOVATE (project code: T1EDK-02990). [ii] This research is also co-financed by Greece and the European Union (European Social Fund- ESF) through the Operational Programme "Human Resources Development, Education and Lifelong Learning" in the context of the project "Strengthening Human Resources Research Potential *via* Doctorate Research" (MIS-5000432), implemented by the State Scholarships Foundation (IKY). (Project No. 2018-050-0502-14406) [iii] Professor T. Vaimakis is thanked for the useful discussion and the recording of TG-DTA/DSC diagrams. [iv] The COST Action CA15114 "Anti-Microbial Coating Innovations to prevent infectious diseases (AMICI)" is thanked for stimulating discussion. (v) S.K.H. acknowledges the Oncology Department of Novartis Hellas S.A.C.I. for the financial support (Project No. 82819).

References

1 N. R. Cozzarelli, DNA gyrase and the supercoiling of DNA, *Science*, 1980, **207**, 953–960.
2 M. Brunner, O. Langer, G. Dobrozemsky, U. Muller, M. Zeitlinger, M. Mitterhauser, W. Wadsak, R. Dudczak, K. Kletter and M. Müller, [18F] Ciprofloxacin, a new positron emission tomography tracer for noninvasive assessment of the tissue distribution and pharmacokinetics of ciprofloxacin in humans, *Antimicrob. Agents Chemother.*, 2004, **48**, 3850–3857.
3 F. Silva, O. Lourenço, J. A. Queiroz and F. C. Domingues, Bacteriostatic versus bactericidal activity of ciprofloxacin in *Escherichia coli* assessed by flow cytometry using a novel far-red dye, *J. Antibiot.*, 2011, **64**, 321–325.
4 M. Mulder, J. C. Kiefte-de Jong, W. H. Goessens, H. de Visser, A. Hofman, B. H. Stricker and A. Verbon, Risk factors for resistance to ciprofloxacin in community-acquired urinary tract infections due to *Escherichia coli* in an elderly population, *J. Antimicrob. Chemother.*, 2017, **72**, 281–289.
5 J. Overgaard, I. Turel and D. E. Hibbs, Experimental electron density study of a complex between copper(II) and the antibacterial quinolone family member ciprofloxacin, *Dalton Trans.*, 2007, 2171–2178.
6 P. Drevensek, T. Zupancic, B. Pihlar, R. Jerala, U. Kolitsch, A. Plaper and I. Turel, Mixed-valence Cu(II)/Cu(I) complex of quinolone ciprofloxacin isolated by a hydrothermal reaction in the presence of L-histidine: comparison of biological activities of various copper-ciprofloxacin compounds, *J. Inorg. Biochem.*, 2005, **99**, 432–442.
7 P. Drevensek, N. Poklar Ulrih, A. Majerle and I. Turel, Synthesis, characterization and DNA binding of mag-

nesium-ciprofloxacin (cfH) complex $[Mg(cf)_2]$ * $2.5H_2O$, *J. Inorg. Biochem.*, 2006, **100**, 1705–1713.

8 I. Milionis, C. N. Banti, I. Sainis, C. P. Raptopoulou, V. Psycharis, N. Kourkoumelis and S. K. Hadjikakou, Silver ciprofloxacin (CIPAG): a successful combination of chemically modified antibiotic in inorganic–organic hybrid, *JBIC, J. Biol. Inorg. Chem.*, 2018, **23**, 705–723.

9 I. Ketikidis, C. N. Banti, N. Kourkoumelis, C. G. Tsiafoulis, C. Papachristodoulou, A. G. Kalampounias and S. K. Hadjikakou, Conjugation of Penicillin-G with Silver(I) Ions Expands Its Antimicrobial Activity against Gram Negative Bacteria, *Antibiotics*, 2020, **9**, 25.

10 M. P. Chrysouli, C. N. Banti, I. Milionis, D. Koumasi, C. P. Raptopoulou, V. Psycharis, I. Sainis and S. K. Hadjikakou, A water-soluble silver(I) formulation as an effective disinfectant of contact lenses cases, *Mater. Sci. Eng., C*, 2018, **93**, 902–910.

11 P. J. Smith, *Chemistry of Tin*, Blackie Academic & Professional, London, 2nd edn, 1997, ISBN 0-7514-0385-7.

12 A. G. Davies, *Organotin Chemistry*, Wiley-VCH Verlag GmbH & Co. KGaA, 2nd edn, 2004.

13 R. Joshi, S. K. Yadav, H. Mishra, N. Pandey, R. Tilak and S. Pokharia, Interaction of triorganotin(IV) moiety with quinolone antibacterial drug ciprofloxacin: Synthesis, spectroscopic investigation, electronic structure calculation, and biological evaluation, *Heteroat. Chem.*, 2018, **29**, 21433.

14 I. Sainis, C. N. Banti, A. M. Owczarzak, L. Kyros, N. Kourkoumelis, M. Kubicki and S. K. Hadjikakou, New antibacterial, non-genotoxic materials, derived from the functionalization of the anti-thyroid drug methimazole with silver ions, *J. Inorg. Biochem.*, 2016, **160**, 114–124.

15 M. K. Stathopoulou, C. N. Banti, N. Kourkoumelis, A. G. Hatzidimitriou, A. G. Kalampounias and S. K. Hadjikakou, Silver complex of salicylic acid and its hydrogel- cream in wound healing chemotherapy, *J. Inorg. Biochem.*, 2018, **181**, 41–55.

16 A. Papadimitriou, I. Ketikidis, M.-E. K. Stathopoulou, C. N. Banti, C. Papachristodoulou, L. Zoumpoulakis, S. Agathopoulos, G. V. Vagenas and S. K. Hadjikakou, Innovative material containing the natural product curcumin, with enhanced antimicrobial properties for active packaging, *Mater. Sci. Eng., C*, 2018, **84**, 118–122.

17 V. A. Karetsi, C. N. Banti, N. Kourkoumelis, C. Papachristodoulou, C. D. Stalikas, C. P. Raptopoulou, V. Psycharis, P. Zoumpoulakis, T. Mavromoustakos, I. Sainis and S. K. Hadjikakou, An Efficient Disinfectant, Composite Material $\{SLS@[Zn_3(CitH)_2]\}$ as Ingredient for Development of Sterilized and Non Infectious Contact Lens, *Antibiotics*, 2019, **8**, 213.

18 F. P. A. Fabbiani, B. Dittrich, A. J. Florence, T. Gelbrich, M. B. Hursthouse, W. F. Kuhs, N. Shankland and H. Sowa, Crystal structures with a challenge: high-pressure crystallisation of ciprofloxacin sodium salts and their recovery to ambient pressure, *CrystEngComm*, 2009, **11**, 1396–1406.

19 C. N. Banti, E. I. Gkaniatsou, N. Kourkoumelis, M. J. Manos, A. J. Tasiopoulos, T. Bakas and S. K. Hadjikakou, Assessment of organotins against the linoleic acid, glutathione and CT-DNA, *Inorg. Chim. Acta*, 2014, **423**, 98–106.

20 S. K. Hadjikakou, M. A. Abdellah, N. Hadjiliadis, M. Kubicki, T. Bakas, N. Kourkoumelis, Y. V. Simos, S. Karkabounas, M. M. Barsan and I. S. Butler, Synthesis, characterization, and biological studies of organotin(IV) derivatives with o- or p-hydroxybenzoic acids, *Bioinorg. Chem. Appl.*, 2009, 542979.

21 M. N. Xanthopoulou, S. K. Hadjikakou, N. Hadjiliadis, M. Kubicki, S. Skoulika, T. Bakas, M. Baril and I. S. Butler, Synthesis, structural characterization, and biological studies of six- and five-coordinate organotin(IV) complexes with the thioamides 2- mercaptobenzothiazole, 5-chloro-2-mercaptobenzothiazole, and 2-mercaptobenzoxazole, *Inorg. Chem.*, 2007, **46**, 1187.

22 M. N. Xanthopoulou, S. K. Hadjikakou, N. Hadjiliadis, M. Schürmann, K. Jurkschat, A. Michaelides, S. Skoulika, T. Bakas, J. Binolis, S. Karkabounas and K. Charalabopoulos, Synthesis, structural characterization and in vitro cytotoxicity of organotin(IV) derivatives of heterocyclic thioamides, 2-mercaptobenzothiazole, 5-chloro-2-mercaptobenzothiazole, 3-methyl-2-mercaptobenzothiazole and 2-mercaptonicotinic acid, *J. Inorg. Biochem.*, 2003, **96**, 425–434.

23 P. Pachori, R. Gothalwal and P. Gandhi, Emergence of antibiotic resistance *Pseudomonas aeruginosa* in intensive care unit; a critical review, *Genes Dis.*, 2019, **6**, 109–119.

24 M. Otto, Staphylococcus epidermidis – the "accidental" pathogen, *Nat. Rev. Microbiol.*, 2009, **7**, 555–567.

25 D. L. Shungu, E. Weinberg and H. H. Gadebusch, Tentative interpretive standards for disk diffusion susceptibility testing with norfloxacin (MK-0366, AM-715), *Antimicrob. Agents Chemother.*, 1983, **23**, 256–260.

26 M. P. Pereira and S. O. Kelley, Maximizing the therapeutic window of an antimicrobial drug by imparting mitochondrial sequestration in human cells, *J. Am. Chem. Soc.*, 2011, **133**, 3260–3263.

27 C. N. Banti and S. K. Hadjikakou, Evaluation of Genotoxicity by Micronucleus Assay in vitro and by Allium cepa Test in vivo, *Bio-Protoc.*, 2019, **9**, e3311.

28 M. Fenech, The micronucleus assay determination of chromosomal level DNA damage, *Methods Mol. Biol.*, 2008, **410**, 185–216.

29 *CrysAlis RED, version 1.171.31.5*, Oxford Diffraction Ltd., 2006 (release 28-08-2006 CrysAlis171.NET), Oxford Diffraction, Crysalis CCD and Crysalis RED, Version p171.29.2, Oxford Diffraction Ltd., Abingdon, Oxford, England, 2006.

30 G. M. Sheldrick, Phase annealing in SHELX-90: direct methods for larger structures, *ActaCrystallogr., Sect.A: Found. Crystallogr.*, 1990, **46**, 467.

31 G. M. Sheldrick, *SHELXL-97, Program for the Refinement of Crystal Structures*, University of Göttingen, Göttingen, Germany, 1997.